catalysts

MDPI

Article

Solar Photocatalytic Degradation of Sulfamethoxazole by TiO_2 Modified with Noble Metals

Ewa Borowska [1,*], João F. Gomes [2], Rui C. Martins [2], Rosa M. Quinta-Ferreira [2], Harald Horn [1,3] and Marta Gmurek [2,4]

1 Karlsruhe Institute of Technology, Engler-Bunte-Institut, Water Chemistry and Water Technology, 76131 Karlsruhe, Germany; harald.horn@kit.edu
2 CIEPQPF—Chemical Engineering Processes and Forest Products Research Center, Department of Chemical Engineering, Faculty of Sciences and Technology, University of Coimbra, 3030-790 Coimbra, Portugal; jgomes@eq.uc.pt (J.F.G.); martins@eq.uc.pt (R.C.M.); rosaqf@eq.uc.pt (R.M.Q.-F.); marta.gmurek@p.lodz.pl (M.G.)
3 DVGW German Technical and Scientific Association for Gas and Water Research Laboratories, Water Chemistry and Water Technology, 76131 Karlsruhe, Germany
4 Department of Bioprocess Engineering, Faculty of Process and Environmental Engineering, Lodz University of Technology, 90-924 Lodz, Poland
* Correspondence: ewa.borowska@kit.edu; Tel.: +49-721-608-4-2788

Received: 16 April 2019; Accepted: 28 May 2019; Published: 30 May 2019

Abstract: Application of solar photocatalysis for water treatment is intensively studied. In this work, we investigated TiO_2 modified with platinum (Pt/TiO_2) and palladium (Pd/TiO_2) using sulfamethoxazole (SMX) as the model contaminant. We considered the following parameters: (i) level of TiO_2 modification with Pt/Pd, (ii) initial concentration of photocatalysts, (iii) geographic location where processes were conducted, and (iv) natural water matrix. The catalysts characterized by SEM, EDX, DRS, and XRD techniques showed successful deposition of Pd and Pt atoms on TiO_2 surface that enabled light absorption in the visible (Vis) range, and therefore caused efficient SMX removal in all tested conditions. A comparison of the rate constants of SMX degradation in various conditions revealed that modification with Pd gave better results than modification with Pt, which was explained by the better optical properties of Pd/TiO_2. The removal of SMX was higher with Pd/TiO_2 than with Pt/TiO_2, independent of the modification level. In the experiments with the same modification level, similar rate constants were achieved when four times the lower concentration of Pd/TiO_2 was used as compared with Pt/TiO_2. Formation of four SMX transformation products was confirmed, in which both amine groups are involved in photocatalytic oxidation. No toxic effect of post-reaction solutions towards *Lepidium sativum* was observed.

Keywords: photocatalytic oxidation; sulfamethoxazole; titanium dioxide modified with noble metals; transformation products; natural sunlight

1. Introduction

Every year numerous studies report on the incomplete removal of anthropogenic contaminants from wastewater during conventional wastewater treatment with activated sludge [1–4]. As a result, the residuals of these compounds are discharged with treated wastewater to receiving waters which can disturb the natural biological balance. Some studies also suggest that the presence of antibiotics in the surface waters or sediments may contribute to the emerging problem of the spread of antibiotic resistance [3,5]. Since the consumption of organic compounds, which are classified in the environment as micropollutants, cannot be decreased, new methods of water or wastewater treatment are studied.

Chemical processes, such as advanced oxidation processes (AOPs), received a lot of attention with respect to their application for water treatment purposes [6–8]. Among them, the semiconductor photocatalysis, especially with titanium dioxide (TiO_2), has been studied in detail, also with regard to the elimination of selected micropollutants in water [9–12]. This inexpensive, stable and nontoxic catalyst gives very good removal efficiencies.

During photocatalytic oxidation, the TiO_2 particle absorbs a photon with energy at least equal to its bandgap and causes excitation of the electrons from the valence band (h^+_{VB}) to the empty conduction band (e^-_{CB}). As a result, electron-hole pairs are created that serve as charge carriers and possess enough redox power to react with dissolved oxygen or water and produce reactive oxidative species (ROS). These reactive species, such as superoxide radicals ($O_2^{\bullet-}$) and hydroxyl radicals, both free ($^{\bullet}OH_{free}$) and adsorbed ($^{\bullet}OH_{ads}$), together with valence band holes (h^+_{VB}) are involved in the degradation of organic pollutants. Unfortunately, apart from the formation of oxidative species, electron-hole recombination takes place which decreases the oxidative potential of the process and hinders formation of new ROS. Due to the wide bandgap of TiO_2 (~3.2 eV) it becomes active only in the UV-A spectrum, and therefore to achieve satisfactory results an application of an UV lamp is necessary ($\lambda < 400$ nm) [13–15]. This obviously generates additional costs and makes the cost efficiency of treatment process questionable.

A search of cheaper and more accessible energy source shifted the focus of the research towards sunlight. Since UV light contributes only in 4–5% in the overall sunlight spectrum, the degradation processes caused by TiO_2 are possible [16], but still most of the solar spectrum remains unused. To benefit from the potential of solar light better, numerous studies on visible (Vis)-light active TiO_2 have been performed [17,18].

One possible modification that results in improved electronic properties is the modification of catalyst surface with noble metals, such as platinum, palladium, gold or silver. Deposition of noble metal nanoparticles on the surface of TiO_2 can improve the degradation of contaminants under visible light due to: (i) increased separation of charge carriers and transport of trapped electrons to oxygen molecules adsorbed on the surface of TiO_2 (which prevents electron-hole recombination), (ii) shifting light absorption towards longer wavelengths as a result of surface plasmon resonance (SPR) of metals (collective electron oscillations), and (iii) resulting modification of surface properties of the photocatalyst [19–21]. As reported in the literature, platinum (Pt) is one of the most active metals for photocatalytic enhancement due to the formation of the highest Schottky barrier between the Pt particles and TiO_2 that prevents the recombination of electric holes and electrons [22]. In the case of palladium (Pd) nanoparticles, high efficiency is explained by high reactivity and selectivity in hydrogenation and Heck reactions that results in higher yields of a conversion to CO_2 and long-term photoactivity [23,24].

Some studies with TiO_2 modified with noble metals have already been conducted. Photocatalytic oxidation with pure and TiO_2 modified with Ag, Au, Pd, and Pt for parabens mixture under UV-A [25], as well as natural sunlight [26], proved that the catalysis enhances the elimination of these compounds as compared with direct photolysis. Improved elimination efficiency was also reported with respect to trimethoprim in the process with Au, Ag, Cu, and Ni nanoparticles deposited on the TiO_2 surface [27]. A study by Ribao et al. [15] showed not only higher efficiency of the degradation process, but also suggested that the major reactive species responsible for degradation are hydroxyl radicals ($^{\bullet}OH$) formed through the transformation of $O_2^{\bullet-}$.

Sulfamethoxazole (SMX), used as a model compound in this study, is one of the main representatives of sulfonamide antibiotics. Due to its bacteriostatic effect towards broad spectrum of gram-positive and gram-negative bacteria, it is often used both in human and in veterinary medicine. Sulfamethoxazole and its metabolites are excreted in urine and directed with wastewater to treatment plants where it is not fully degraded [28].

SMX has already been used to test the efficiency of a sunlight mediated process with titanium dioxide modified for instance with tungsten (WO_3/TiO_2) [29], copper (Cu/TiO_2) [30,31], gold (Au/TiO_2),

and silver (Ag/TiO_2) [31]. For this purpose also non-TiO_2 based catalysts were investigated, such as flower-like bismuth oxide (Bi_2O_3) [32], cuprous oxide-reduced graphene oxide (Cu_2O/rGO) [33], composites of silver orthophosphate with tungsten oxide (Ag_3PO_4/WO_3), [34] and many others.

Therefore, in our study we aim to investigate sunlight-mediated photocatalytic degradation of sulfamethoxazole with titanium dioxide that is modified with the noble metals, palladium, and platinum. The study was divided into the following tasks: (i) characterization of Pd/Pt-modified TiO_2, (ii) description of SMX adsorption on the catalyst surface, (iii) testing the effect of level of catalyst modification and initial concentration of catalyst on SMX photo-oxidation, (iv) comparison of the efficiency of photocatalytic degradation in Portugal and Germany, (v) comparison of the process efficiency in pure solutions and environmental samples. Keeping in mind that an ideal catalyst does not only absorb Vis-light and efficiently remove micropollutants, but should also cause high mineralization and/or a formation of nontoxic transformation products, we investigated the formation of the latter, and finally assessed their potential toxic effect in a post-reaction solution towards *Lepidium sativum*. Completion of all these tasks gave a detailed answer about the potential of the solar photocatalysis and indicated a direction for further research.

2. Results and Discussion

2.1. Characterization of the Photocatalysts

SEM images of successfully deposited Pd and Pt onto TiO_2 are depicted in Figure 1. Deposition of Pd particles resulted in the homogeneous distribution of the particles on the catalyst surface (Figure 1a). In the case of Pt, its particles were incorporated on the TiO_2 surface in an irregular manner (Figure 1b). More SEM pictures are found in Supporting Information (SI) Figures S1 and S2.

Elemental composition of catalysts is shown on the corresponding energy-dispersive X-ray (EDX) spectra (Figure 1c). It should be noted that chlorine was not found in the Pd/TiO_2 sample. This clearly indicates that Cl^- ions from the precursor ($PdCl_2$) were efficiently removed during the washing procedure applied after synthesis. In the case of Pd/TiO_2, chlorine was found in low concentration (0.29% weight, 0.20% atomic). However, although the concentration is low, it is relatively high with respect to metal concentration, and as reported by Leong et al. [35], it can potentially result in suppressing the photocatalytic activity.

Catalysts used in the study were characterized also by UV-Vis diffuse reflectance (DRS) spectrophotometry. As shown in Figure 1d, all catalysts exhibit very strong absorption below 400 nm which can be explained by the property of titanium to absorb UV light. However, above 400 nm, (visible light region) only Pd/TiO_2 and Pt/TiO_2 exhibit a significant absorption. As discussed above, this broad absorption band may be attributed to the surface plasmon resonance of noble metal nanoparticles [19,35].

Moreover, Pd/TiO_2 exhibits better absorption characteristics in the Vis-light range than Pt/TiO_2 (Figure 1d). This can be attributed to the width of the bandgaps as shown in Figure 1e (Tauc plot). Direct bandgap of pure TiO_2 (3.38 eV) was reduced to 2.92 eV and 3.18 eV for 1% Pd/TiO_2 and 1% Pt/TiO_2, respectively (Figure 1e). Since Pd/TiO_2 has narrower bandgaps (direct, indirect) than Pt/TiO_2, it performs in the Vis-light range better, increasing the efficiency of the photocatalysis. Determined values of indirect bandgap of TiO_2 (3.27eV) and Pt/TiO_2 (2.71 eV) (Figure 1e) are consistent with the literature data for TiO_2 [13–15] and for Pt/TiO_2 [36,37].

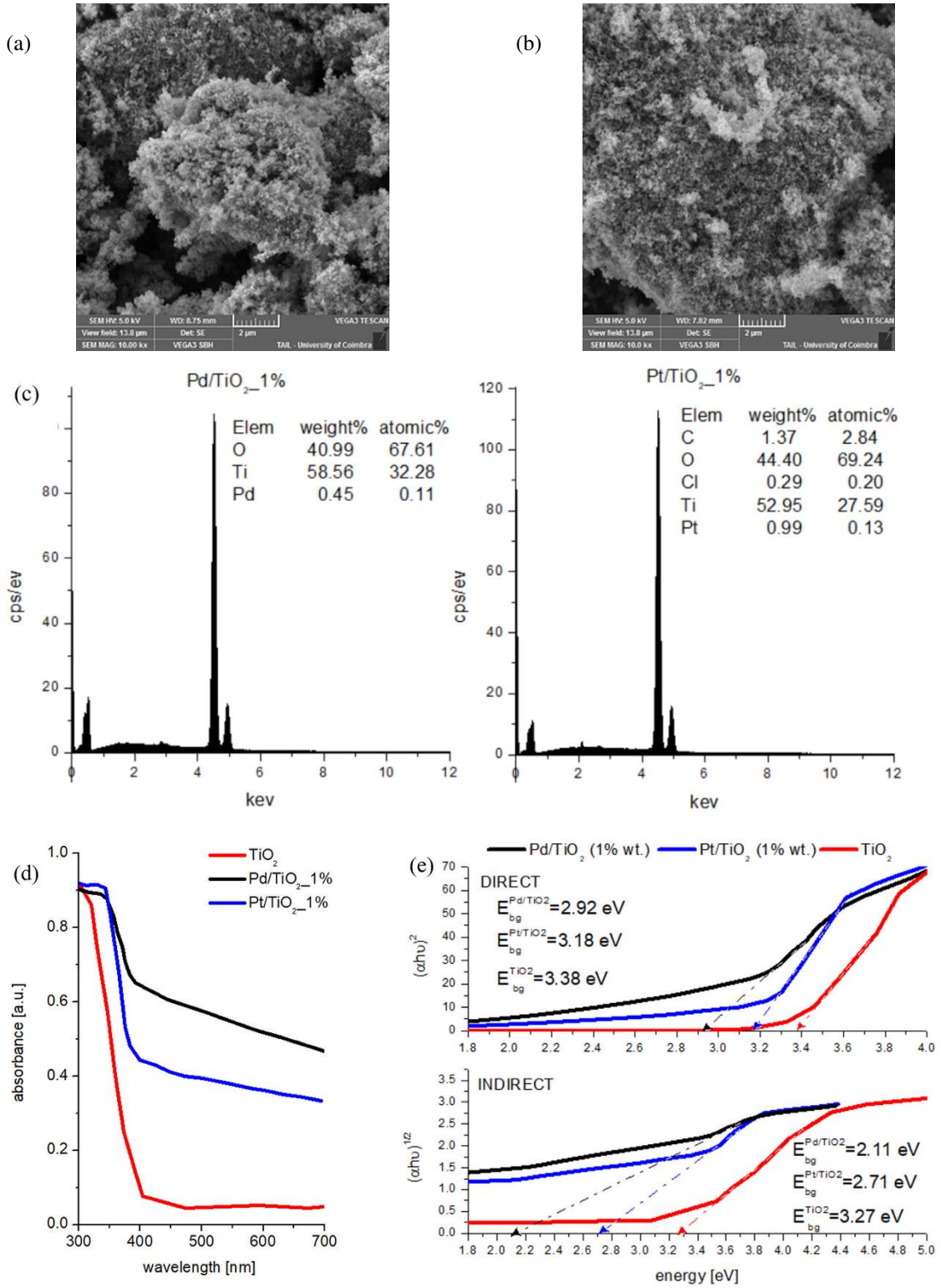

Figure 1. Characterization of TiO_2 modified with Pd and Pt: (**a**) SEM image of 1% Pd/TiO_2; (**b**) SEM image of 1% Pt/TiO_2; (**c**) EDX spectra of 1% Pd/TiO_2 and 1% Pt/TiO_2; (**d**) UV-Vis absorption spectra of TiO_2 (P25), 1% Pd/TiO_2, and 1% Pt/TiO_2; (**e**) determination of the direct and indirect bandgaps.

It is well known that structure modification of TiO_2 with platinum and palladium nanoparticles (NPs) improves the quantum yield of photoconversion, as well as it shifts the light absorption of wide bandgap semiconductors to the Vis-light range [19]. Pure TiO_2 is an n-type semiconductor and

the n/p transition depends on the type and concentration of the metal used for modification [38,39]. The conduction band (CB) or valence band (VB) of the n-type semiconductor bends upwards to the metal with respect to their relative work functions [40]. Noble metal has a higher work function than TiO_2 which induces the formation of a Schottky barrier [41] In principle, the Schottky barriers are formed on the contact interface between a metal and a semiconductor, and they equalise the Fermi edges of the metal and the TiO_2. Pt has a larger work function (5.65 eV) than Pd (5.12 eV) [42], and therefore it is able to produce the higher Schottky barrier resulting in the higher activity[19]. The Pt-NPs modification enhances photocatalytic activity due to capturing of electrons, longer electron-hole pair separation, lifetime hindering of the electron-hole pairs recombination, and increasing the transfer of holes and electrons to O_2 adsorbed on the TiO_2 surface [22,43]. On the other hand, modification of TiO_2 with Pd-NPs improves photocatalytic activity via the stimulation of the transfer of photogenerated electrons from the TiO_2 conduction band to the Pd-NPs conduction band. This results in accumulation of the holes in the TiO_2 valence band and reduction of electron-hole pair recombination [43,44].

X-ray diffraction (XRD) measurement confirmed the occurrence of the expected crystallographic forms of the modified TiO_2 (Table S1). The ratio between anatase and rutile phases was 89/11 and 80/20, for Pd/TiO_2 and Pt/TiO_2, respectively, which proved that surface modification with noble metals did not significantly change the basic structure of TiO_2-P25. The analysis of lattice constants confirmed the tetragonal structure of anatase ($a = b \neq c$). Furthermore, the data showed that atoms of metals were not built into the anatase structure, but deposited on the surface of TiO_2. Reflections from Pd were also noted, however, their intensity was too low to be able to analyze the size of crystallites.

It is worth mentioning that the crystalline structure of the both modified-TiO_2 catalysts (Figure S3) remained in anatase phases TiO_2 , since two most obvious diffraction peaks are observed at 25.3° and 48.0°. The obtained pattern also proved the absence of the brookite phases, while rutile was clearly visible (the strongest rutile reflect was observed at 27.5°).

2.2. Adsorption Experiment

In order to understand the adsorption process of SMX on the catalysts, the isothermal adsorption experiments were carried out.

As shown in Figure S4a (fitting curves according to Langmuir model) and in Table 1, the Langmuir model can well describe the adsorption on the TiO_2-based catalysts (high R^2 values). Values of both maximal loading (q_{max}) and Langmuir constant (K_L) clearly indicate that modification of the TiO_2 surface with noble metal nanoparticels, significantly increases adsorption properties of the materials as compared with non-modified titanium dioxide. Furthermore, when the catalyst surface was modified with palladium, much more SMX was adsorbed as compared with modification with platinum. The maximal loadings were determined as 6.31 ± 0.43 mg_{SMX}/g_{cat} and 21.60 ± 6.80 mg_{SMX}/g_{cat} for Pt/TiO_2 and Pd/TiO_2, respectively, which is 2.2 and 7.7 times more than the maximal loading of non-modified TiO_2.

Table 1. Maximal loading of SMX of catalyst surface (q_{max}) and corresponding Langmuir constants (K_L).

	q_{max} 10^{-3} [mg_{SMX}/g_{cat}]	K_L [dm^3/mg]	R^2
TiO_2	2.82 ± 0.39	1.454 ± 0.412	0.89
Pt/TiO_2	6.31 ± 0.43	0.956 ± 0.043	0.93
Pd/TiO_2	21.60 ± 6.80	1.562 ± 0.830	0.97

In additional sorption experiments, the equilibrium time of 10 min was determined for adsorption of SMX on the catalysts surface (SI Figure S4b). However, due to experimental preparation, normally the contact of catalysts with SMX before the beginning or sunlight exposure was around 1 h.

2.3. Photocatalytic Degradation of Sulfamethoxazole

2.3.1. Efficiency Comparison of Modified and Non-Modified TiO_2

Preliminary experiments (concentration of catalyst ~50 mg/L) comparing the performance of SMX photodegradation showed that deposition of noble metal on the surface of TiO_2 drastically changed its properties. This is also in agreement with the results of catalysts characterization. As depicted in Figure 2, 30 min of sunlight exposure did not cause significant decay of SMX (<5%) when TiO_2 was applied, which was expected, since TiO_2 is active only in UV spectrum. However, when TiO_2 was modified with Pt, the same duration of sunlight exposure resulted in almost 90% of SMX removal. Almost complete elimination of SMX was noted for Pd/TiO_2 just after 10 min of sunlight exposure. Higher process efficiency for Pd/TiO_2 as compared with Pt/TiO_2 can be explained by better light absorption properties (Figure 1d), higher adsorption on the catalyst surface (Figure S4a, Table 1), as well as potentially inhibiting presence of chloride residual on the catalyst surface (Figure 1c). Pseudo-first order rate constants of these processes and corresponding half-lives are collected in Table 2. The calculated values of pseudo-first order rate constants for the processes with Pt/TiO_2 and Pd/TiO_2 are 38 and 260 times higher, respectively, than for the process with non-modified TiO_2 with the same sunlight conditions. This means that to observe 50% decay of SMX with TiO_2 almost 4 h of sunlight exposure are needed, whereas, when Pd/TiO_2 or Pt/TiO_2 are used the same abatement can be achiever after only 1.3 min and 9.1 min, respectively.

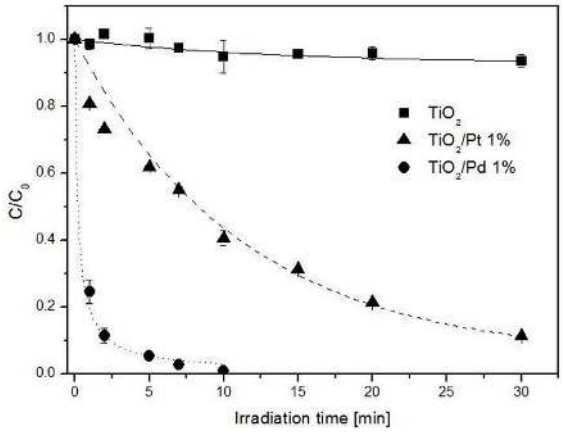

Figure 2. Comparison of solar-driven photodegradation of SMX using (■) TiO_2, (▲) Pt/TiO_2, (1%), (●) Pd/TiO_2 (1 %). C_{cat} = ~50 mg/L, C_{SMX_0} = 1 mg/L.

Table 2. Pseudo-first order rate constants and half-lives for the solar-driven phototransformation of sulfamethoxazole ith TiO_2 modified with noble metal.

Aim of the Experiment	Type of Catalyst	Surface Modification Level (%)	Exact Concentration of Catalyst (mg/L)	Pseudo-First Order Rate Constant k' (10^{-2} 1/min)	Half-Life $t_{1/2}$ (min)
Effect of TiO_2 surface modification with noble metal	TiO_2	-	53.2	0.2 ± 0.1	284.5 ± 64.4
	Pd/TiO_2	1.0%	56.7	52.1 ± 5.1	1.3 ± 0.2
	Pt/TiO_2	1.0%	46.7	7.6 ± 0.1	9.1 ± 0.1
Effect of surface modification level	Pd/TiO_2	0.1%	29.3	7.5 ± 0.8	9.3 ± 1.1
		0.5%	27.0	11.0 ± 1.0	6.4 ± 0.9
		1.0%	30.0	50.6 ± 3.0	1.4 ± 0.1
	Pt/TiO_2	0.1%	27.3	2.0 ± 0.1	33.8 ± 1.2
		0.5%	24.1	2.1 ± 0.1	33.3 ± 2.5
		1.0%	28.7	2.0 ± 0.1	34.2 ± 0.9
Effect of catalyst concentration	Pd/TiO_2	1.0%	23.5	14.1 ± 1.5	5.0 ± 0.1
		1.0%	56.8	52.1 ± 5.1	1.3 ± 0.2
		1.0%	76.8	43.9 ± 3.7	1.6 ± 0.2
		1.0%	114.4	46.2 ± 4.3	1.5 ± 0.2
	Pt/TiO_2	1.0%	26.5	3.8 ± 0.2	18.5 ± 1.3
		1.0%	46.7	7.6 ± 0.1	9.1 ± 0.1
		1.0%	81.3	14.9 ± 0.3	4.7 ± 0.2
		1.0%	117.1	20.3 ± 0.4	3.4 ± 0.1

2.3.2. Effect of Surface Modification Level

To investigate the relation between the extent of TiO_2 modification and degradation of SMX, photodegradation was performed using Pt/TiO_2 and Pd/TiO_2, modified with 0.1%, 0.5%, and 1% noble metal. In order to have a closer look into the differences between catalysts' performance, their concentration was decreased to ~25 mg/L. Pseudo-first order rate constants, as well as corresponding half-lives, are presented in the Table 2. The curves with average SMX abatement are presented in the SI Figures S5 and S6.

In the case of Pt/TiO_2, pseudo-first order rate constants are in a comparable range, between 0.020 1/min and 0.021 1/min, with the corresponding half-lives ranging from 33 to 34 min. This indicates, that a surface modification level in the range of 0.1% to 1.0% does not have an effect on the degradation process efficiency.

A different trend was observed in the experiments with Pd/TiO_2. For this catalyst, the higher a surface modification was introduced, the higher pseudo-first order rate constant was achieved, (i.e., *k*' for surface modification level of 0.1% was calculated as 0.075 1/min), whereas, for 1% it was 0.506 1/min. Such a change could be explained by the higher adsorption capacity of the catalysts modified with palladium, and also the actual percent of TiO_2 modification with the noble metal.

The XPS survey spectra of 1% Pt/TiO_2 and 1% Pd/TiO_2 are depicted in Figure S7 in SI. For both catalysts, two feature peaks of Ti 2p states can be recognized (Figure S4a,c), at 458.8 eV and at 464.7 eV for Ti 2p3/2 and Ti 2p1/2, respectively, with a peak separation at 5.9 eV assigned to Ti (IV) (titanium in the IV oxidation state). A comparison of Figure S7b,d revealed that the Pt signal is weaker than the Pd signal, however, strong enough to assign them to their chemical states.

As shown in Figure S7b, typical XPS peaks of 4f Pt signal were observed. Deconvolution of Pt 4f spectrum can be explained by the occurrence of several Pt chemical states. The peak at 76 eV can be attributed to PtO which is in agreement with the existing literature. However, due to the relatively wide signal between 71 and 74 eV, we believe that both Pt(0) and $Pt(OH)_2$ could be present, which are normally detected at 71 eV and 72 eV, respectively.

The XPS profile of monometallic 1% Pd/TiO_2 (Figure S7d) was dominated by a peak at 337.7 eV that corresponds to the Pd–Cl bonds. The peak recorded at 336 eV was assigned to PdO.

The relative concentrations of elements of various TiO_2 modification levels with Pd and Pt are provided in Table 3. The analysis confirmed that Pt is present in the structure of catalyst, even at the lowest modification level. The catalyst described as 0.1% Pt/TiO_2 showed the atomic Pt content (atom%) of 0.08%, which is near the expected value. The XPS measurements of catalyst 0.5% Pt/TiO_2 indicated that only 0.13 atom% of Pt was successfully deposited on the TiO_2 surface. In the case of 1% Pt/TiO_2, the detected Pt concentration was closer to the expected value, i.e., 0.61 atom% (Table 3). The differences in targeted and actual percentages of modifications are the results of lower than assumed yield of the photodeposition method. The same observation was made for Pd/TiO_2, where only 0.23 atom% Pd, instead of assumed 0.5% was detected (Table 3). Moreover, the SEM analysis of Pt/TiO_2 catalysts (0.1, 0.5, and 1%) confirmed that roughness and shape do not change with the increase of noble metal loading for 0.1 and 0.5 wt%, whereas, for 1% Pd the agglomerates were observed (Figure 1a, Figures S1 and S2). It was also observed that morphology changed for higher Pd loading and this promoted formation of microspheres.

Table 3. Relative elemental concentrations obtained from the XPS composition analysis.

Catalysts	O (%)	Ti (%)	C (%)	Pt Content (atom%)	Pd Content (atom%)
Pt/TiO_2_0.1%	48.57 ± 0.43	21.11 ± 0.17	30.25 ± 0.59	0.08 ± 0.01	-
Pt/TiO_2_0.5%	48.70 ± 0.55	20.73 ± 0.01	30.46 ± 0.54	0.13 ± 0.01	-
Pt/TiO_2_1%	46.74 ± 0.27	18.13 ± 0.04	34.23 ± 0.13	0.61 ± 0.01	-
Pd/TiO_2_0.5%	55.88 ± 0.05	23.66 ± 0.62	20.24 ± 0.66	-	0.23 ± 0.01
Pd/TiO_2_1%	54.95 ± 0.41	23.40 ± 0.32	20.95 ± 0.05	-	0.70 ± 0.02

2.3.3. Effect of Initial Concentration of Catalyst

The solar photocatalytic degradation of SMX was also assessed with respect to the applied concentration of modified catalysts. For this reason, four concentrations were investigated: ~25 mg/L, ~50 mg/L, ~75 mg/L, and ~120 mg/L, using modified TiO_2 at a surface modification level of 1%. This modification level was chosen because though it did not have significantly better performance with respect to lower modification levels of Pt/TiO_2, it had high impact in the case of Pd/TiO_2. For the following parts of the study, we wanted to maintain the conditions of these two photocatalytical processes as consistent as possible, and therefore a modification level of 1% for both types of photocatalysts, in our opinion was the most reasonable.

The results showed that for Pd/TiO_2 the effect of catalyst concentration is apparent only for the lowest tested concentration of ~25 mg/L (Table 2, Figure S8). The k' was in this case 0.141 1/min, whereas for all the higher concentrations, k' values were twice as high, however, in the relatively narrow range of 0.439–0.521 1/min. This could mean that with concentrations above 50 mg/L, the saturation occurs and further increase of the catalyst concentration does not improve the treatment process efficiency.

For Pt/TiO_2, the effect of catalyst concentration on the reaction rate was much stronger (Figure S9). As depicted in Figure S10, there is an ideal linear dependence between applied Pt/TiO_2 concentration and k' ($R^2 = 0.99$). In this case, saturation of the catalyst with the tested compound did not occur. Perhaps a continuous increase of catalyst concentration would result in even higher process efficiency. However, it should be noted, that using Pt/TiO_2 at the concentration of ~80 mg/L, gave comparable photocatalysis efficiency as Pd/TiO_2 at the concentration ~25 mg/L ($k'_{Pt/TiO_2} = 0.149$ 1/min, $k'_{Pd/TiO_2} = 0.141$ 1/min).

2.3.4. Effect of Water Matrix and Sunlight in Germany and Portugal

The photocatalytic efficiency was compared in two different geographic locations, using both aqueous solutions and natural river water spiked with SMX. The determined kinetics parameters are presented in Table 4 and the degradation curves achieved in these experiments are presented in SI Figure S11.

Pseudo-first order rate constants indicate that the photocatalytic degradation of SMX in aqueous solution was slightly slower in Portugal as compared with the same experiments performed in Germany. Such observation can be explained by the difference in sunlight exposition. Radiometer measurements showed that the average irradiance for experiments performed in Karlsruhe was around 430.1 W/m^2 and in Coimbra 326.5 W/m^2 (in the range 250–700 nm).

Table 4. Pseudo-first order rate constants and half-lives for the solar phototransformation of sulfamethoxazole with TiO_2 modified with noble metal in aqueous solutions and river water.

Country	Type of Matrix	Type of Catalyst	Pseudo-First Order Rate Constant (10^{-2} 1/min)	Half-Life Time (min)
Germany	Aqueous solution	Pd/TiO_2	14.1 ± 1.5	5.0 ± 0.1
		Pt/TiO_2	3.8 ± 0.2	18.5 ± 1.3
	Alb river (TOC = 5.5 mg/L)	Pd/TiO_2	2.1 ± 0.1	33.3 ± 0.7
		Pt/TiO_2	0.8 *	86.6 *
Portugal	Aqueous solution	Pd/TiO_2	12.7 ± 0.2	5.4 ± 0.1
		Pt/TiO_2	2.4 ± 0.2	27.4 ± 1.4
	Mondego river (TOC = 6.4 mg/L)	Pd/TiO_2	4.4 ± 0.2	15.9 ± 1.2
		Pt/TiO_2	1.5 ± 0.2	47.6 ± 6.9

Conditions: surface modification level 1%, catalyst concentration ~25 mg/L; * single measurement.

The tests conducted in river water showed an influence of the water matrix on the degradation rate. In Alb river (TOC = 5.5 mg/L), the processes involving any of the investigated catalysts were roughly 5–7 times slower, as compared with the reaction rate in aqueous solutions. On the other hand, though the content of organic matter in the Mondego river was in a similar range (TOC = 6.4 mg/L),

the reaction rate constants were affected to a lower extend. The *k'* values between reactions in aqueous solutions and river water spiked with SMX differed roughly by a factor of two.

A comparison of photocatalysis efficiency in two types of river water revealed that despite worse irradiance conditions in Portugal, both Pd/TiO_2 and Pt/TiO_2 performed better in SMX degradation in the Mondego river as compared with the Alb river. The *k'* values for Pd/TiO_2 and Pt/TiO_2 in Mondego river were two times higher as compared with the Alb water. This suggests that not only the concentration of organic content influences the photocatalytic degradation, but possibly, also its composition and presence of other water constituents, although they were not studied within this work.

2.4. Mineralization

Mineralization was assessed as a decay of dissolved organic carbon (DOC). As shown in Figure 3a, although after 60 min of photocatalytic degradation with Pd/TiO_2 no SMX was detected in the samples, observed mineralization was around 45 ± 2%. In the process with Pt/TiO_2 (Figure 3b), the same light conditions (the same exposure and duration of radiation) resulted in a decrease of SMX concentration by 90 ± 1%, and at the same time mineralization of 29 ± 10%.

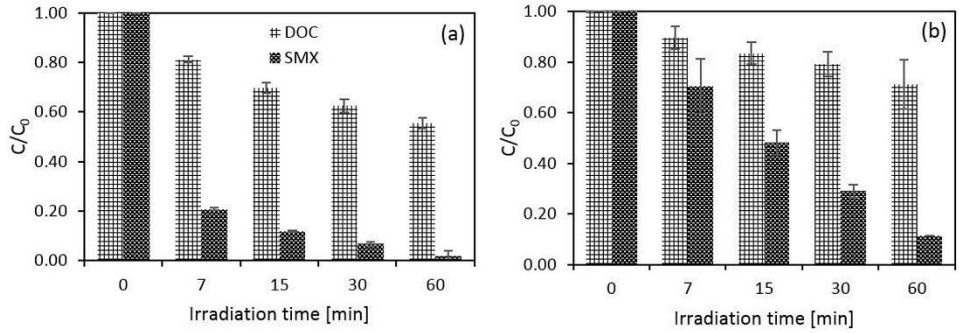

Figure 3. Mineralization and SMX abatement during solar-driven photocatalytic degradation with (**a**) Pd/TiO_2; (**b**) Pt/TiO_2 (modification level 1%, C_{cat} = ~25 mg/L, C_{SMX_0} = 1 mg/L).

The achieved mineralization was still better than previously reported for TiO_2. A study by Abellán et al. [45] where the abatement of SMX in the UV/TiO_2 process was investigated showed TOC removal, in the range of 23%, when 0.5 g TiO_2 was used. In our experiment a concentration of 25 mg/L was used. This indicates that the modification of TiO_2 with noble metals drastically descreases the demand of the catalyst, here, by a factor of 20. The modification of TiO_2 with tungsten investigated by Ioannidou et al. [29] also did not result in higher mineralization (~28% after 6 h of irradiation).

The catalysts used in this study were previously investigated with respect to parabens [25,26]. In this study, mineralization of parabens with 0.5% Pd/TiO_2 was only 25% and less than 10% after exposure to UVA (3 h) and sunlight (2 h), respectively, when 70 mg/L of catalyst was applied. In our study, almost three times lower concentration of the catalysts resulted with higher mineralization in a much shorter time, indicating that SMX can be transformed more easily.

High elimination of SMX with relatively low mineralization indicates the need for the investigation of the transformation products (TPs).

2.5. Transformation Products (TPs)

Analysis of transformation products confirmed formation of four compounds (Figure 4). These structures were already reported by Gmurek et al. [46] during photolysis of SMX with natural sunlight. As shown in Figure 4, the detected transformations of the SMX molecule (m/z (+) 254.0) occurred on both amine groups.

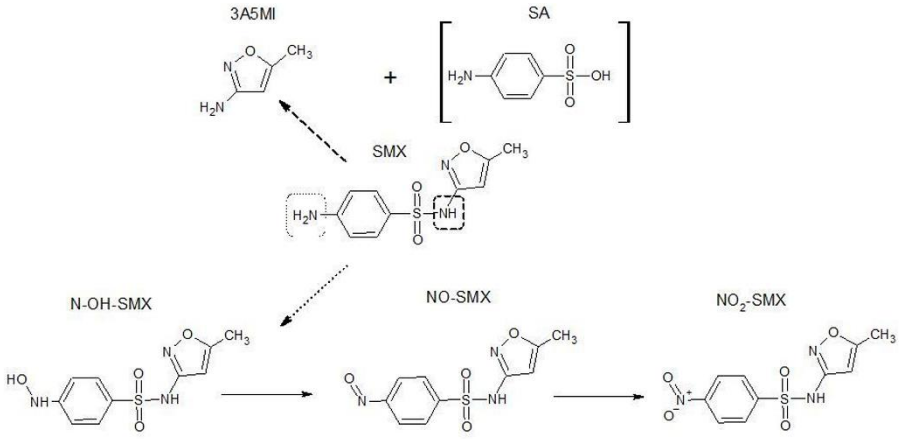

Figure 4. SMX TPs identified during photocatalytic degradation with Pt/TiO_2 and Pd/TiO_2.

The signal of m/z (+) 270.1 indicated addition of one atom of oxygen to the molecule of the parent compound, which was explained by oxidation of primary amine resulting in formation of N-hydroxy-sulfamethoxazole (N-OH-SMX). Further oxidation led to signal m/z (−) 265.9 corresponding to 4-nitroso-sulfamethoxazole (NO-SMX) and eventually to signal m/z (−) 282.0 assigned to 4-nitro-sulfamethoxazole (NO_2-SMX).

Figure 5 illustrates formation of all the found TPs. As shown in the figure, all TPs were detected in both discussed photocatalytic processes, however, their evolution took place faster in the reaction with Pd/TiO_2 (Figure 5a) as compared with the reaction with Pt/TiO_2 (Figure 5b). Normalization to the maximal peak area, which was found during the experiment, allowed distinction of the order in which TPs were formed, which was also considered in the preparation of Figure 4.

Interestingly, NO_2-SMX, which is the most oxidized compound of confirmed SMX TPs, was detected with the highest signal intensity after 30 min of the experiments with Pt/TiO_2, whereas, after the same duration of exposure to sun, the signal of this compound was almost undetectable any more. This could explain the higher degree of mineralization for photocatalysis with Pd/TiO_2, however, it can also suggest formation of subsequent TPs generations that could not be covered by this study.

Another type of SMX transformation involved the secondary amine. Such transformation led to the formation signal m/z (+) 99.1, which was assigned to 3-amino-5-methylisoxazol (3A5MI), as a result of bond cleavage between sulphur and nitrogen. As shown in Figure 5a, the signal of 3A5MI was the most intense after 10 min of the reaction with Pd/TiO_2, and after 20 min of the reaction with Pt/TiO_2. Afterwards, it started slowly to decrease, leading to smaller molecules and perhaps eventually even to mineralization.

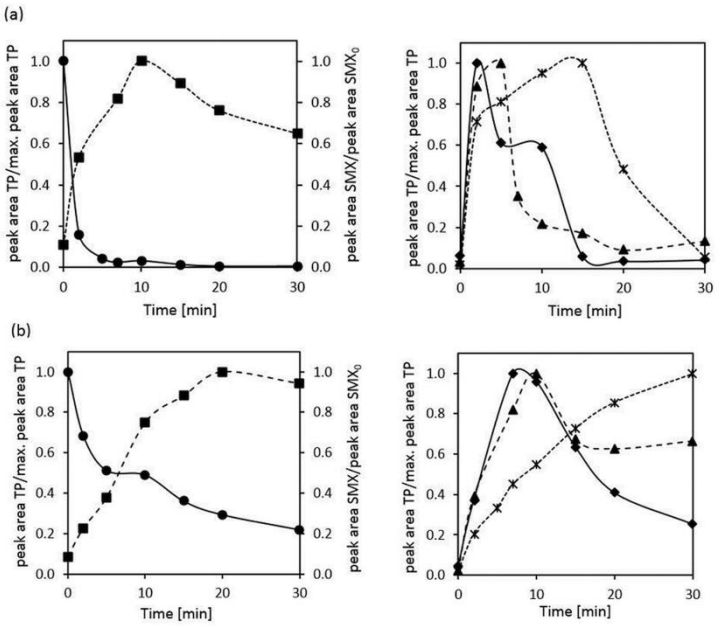

Figure 5. Semi-quantitative determination of SMX and its TPs formed during photocatalytic oxidation with (**a**) Pd/TiO_2; (**b**) Pt/TiO_2 (surface modification level 1%, C_{cat} = ~ 25 mg/L): (●) SMX, (■) 3A5MI, (♦) N-OH-SMX, (▲) NO-SMX, (*) NO_2-SMX.

We expected that parallel to the formation of 3A5MI, the signal of m/z (−) 172.0 corresponding to sulfanilic acid (SA) could be observed. However, such a signal was not detected in any of the samples. This means that this compound is unstable in the oxidative conditions and it undergoes further transformations.

4-Hydroxy-SMX (m/z (−) 252.9, OH-SMX) was found mainly in the unirradiated samples, indicating impurities of the SMX solution with oxidized SMX. After the initiation of the photocatalytical processes with Pt/TiO_2 and Pd/TiO_2, the signal intensity decreased after the first few minutes (data not shown), suggesting that this compound cannot be considered as a transformation product. In our previous study [46] we reported on the formation of this compound in a ng/L concentration range during photolysis of 100 mg/L SMX solution, proving that such transformation is not relevant.

The signals belonging to sulfacetamid (m/z (+) 214.9, SFAA), acetyl-sulfamethoxazole (m/z (+) 296.0, acetyl-SMX), N-hydroxy-acetyl-SMX (m/z (+) 312.0, OH-acetyl-SMX), and sulfanilamide (m/z (+) 172.8, SAD) were also found, however, also with very low signal intensity (data not shown) which made the formation of these compounds questionable. In the case of OH-SMX, as also stressed in previous work [46], these compounds were detected only in the very high initial concentration of SMX. Structures of these compounds are collected in SI Table S2.

All proposed TPs were confirmed using commercial standards for comparison of their fragmentation patterns and retention times. Taking into consideration the confidence system of identification of unknown compounds [47], all of the TPs discussed here belong to level 1 which corresponds to the confirmed structure. The MS^2 spectra of SMX and its TPs are presented in SI Figures S12–S16.

2.6. Ecotoxicity

Since total mineralization was not achieved during photodegradation (Figure 3), and the formation of TPs was confirmed (Figures 4 and 5), the toxicity of the solution after 60 min of photocatalytic treatment was compared to the toxicity of unirradiated SMX solution.

Toxicity towards *Lepidium sativum* was expressed as the germination index (GI, %). Values in the range of 80–100% mean that the solutions do not affect germination and the lower value of GI, the higher the phytotoxicity.

As shown in Table 5, GI for the initial SMX solution (not exposed to treatment) was 43 ± 4%, which according to Trautmann and Krasny [48] corresponds to high phytotoxicity. On the other hand, GI of the SMX solutions after the photocatalytic process with Pd/TiO_2 and Pt/TiO_2 were calculated as 93 ± 10% and 110 ± 16%, respectively, clearly indicating that post-reaction SMX solutions exhibit no phytotoxicity towards the tested bioindicator. The monitored SMX concentration during the experiment (SI Figure S17) showed, after the process, that 95% and 80% of SMX decay was reached when Pd/TiO_2 and Pt/TiO_2, respectively, was applied. This means that observed low toxicity could be explained by the low andvery low concentrations of SMX in the medium and the harmless presence of SMX TPs.

Table 5. Seed germination index (GI) before and after the solar photocatalytic oxidation process.

Type of Solution	Germination Index (± SE) [%]
Initial SMX solution	43 (±4)
Solution after treatment with Pd/TiO_2	93 (±10)
Solution after treatment with Pt/TiO_2	110 (±16)

SE: Standard Error.

Toxicity of post-reaction mixture of SMX was tested by Gmurek et al. [46] in a luminescence test and growth inhibition tests. Their results showed that there is a toxic effect on luminescence attributed most likely to TPs, and at the same time growth inhibition activity was observed to decline over irradiation time.

An increase of GI after irradiation of the SMX solution determined for *Lepidium sativum* was in agreement with the results of Gomes et al. [25] observed in the process of TiO_2 modified with noble metals used for the treatment of parabens.

3. Materials and Methods

3.1. Chemical and Reagents

Sulfamethoxazole (SMX), sulfacetamid (SFAA), acetyl-sulfamethoxazole (acetyl-SMX) and sulfanilamide (SAD) were purchased at Dr. Ehrenstorfer GmbH (Augsburg, Germany). 3-amino-5-methylisoxazole (3A5MI) and sulfanilic acid (SA) were obtained from Sigma Aldrich (Seelze, Germany). Sulfamethoxazole-d_4, 4-nitro-sulfamethoxazole (NO_2-SMX), 4-nitroso-sulfamethoxazole (NO-SMX), and N-hydroxy-sulfamethoxazole (N-OH-SMX) were purchased at Toronto Research Chemicals (Toronto, Canada). 4-hydroxy-sulfamethoxazole (4-OH-SMX) and N_4-hydroxy-acetylsulfamethoxazole (OH-acetyl-SMX) were synthesized as previously described [49]. A commercial form of TiO_2 (P25, crystalline composition: 80% anatase, 20% rutile, surface area 50 m^2/g) was obtained from Evonik (Essen, Germany.) For analysis, 2-propanol was purchased at Merck (Darmstadt, Germany). All solvents, HPLC water (VWR), acetonitrile (Merck), formic acid (Merck), were analytical grade (≥99%). The experimental solutions were prepared using ultrapure water. The catalysts, Pd/TiO_2 and Pt/TiO_2, used in the study were prepared by UV-reduction of Pt^{4+} and Pd^{2+} used as a chlorides in the TiO_2 (P25) suspension using the method described elsewhere [25].

3.2. Characterization of Photocatalysts

The microstructural analysis of the surfaces was performed using a TESCAN VEGA 3 SBH (Tescan, Brno, Czechia) Easy Probe Scanning Electron Microscopy (SEM) with a tungsten heated cathode. The SEM images were acquired with a working tension of 5 kV and using the secondary electrons detector. The energy dispersion X-ray spectroscopy (EDX) analysis (system Quantax with Nano XFlash detector, Bruker Company, Berlin, Germany), coupled with the scanning electron microscopy, was used to analyze the elements composition of the samples.

The optical properties of the samples were characterized by an ultraviolet/visible diffuse reflectance (DRS) spectrophotometer (Evolution 220, Thermo Scientific, Waltham, MA, USA), in which $BaSO_4$ was employed as the internal reflectance standard.

The crystal structure of photocatalysts was determined from the XRD pattern measured in the range of 2θ = 20–80° using an X-ray diffractometer (Xpert PRO-MPD, Philips, Eindhoven, Netherlands) with Cu target (λ = 1.542 Å). The lattice parameters were estimated by the LeBail method using a FullProf package.

3.3. Adsorption Experiment

The batch adsorption experiment was carried out in a set of amber glass bottles (100 mL) containing SMX solution of concentration ranging from 0.1 mg/L to 5 mg/L, and an addition of catalyst, placed in a thermostatic shaking incubator at 25 °C with 150 rpm. After 60 min of reaction, the solutions were filtered via syringe cellulose acetate filters (pore size 0.45 µm, Macherey-Nagel GmbH & Co. KG, Düren Germany) to remove catalyst and the concentration of SMX in the filtrate was measured. All experiments were performed twice at pH 6.2 (pH of MilliQ water). Sorption was tested with an addition of catalysts at the concentration in the range 26–29 mg/L, 24–28 mg/L and 24–27 mg/L for TiO_2, 1% Pt/TiO_2, and 1% Pd/TiO_2, respectively. The observed adsorption was described using the Langmuir approach.

3.4. Sunlight Conditions

Irradiation experiments were performed using natural sunlight in June 2017 in Karlsruhe, Germany (49° 0′ 34″ N, 8° 24′ 15″ E) and in Coimbra, Portugal in August 2018 (40° 12′ 12″ N, 8° 24′ 37″ W). The characterization of the weather has been made based on the data available from The Deutscher Wetterdienst (DWD) (https://www.dwd.de/) (SI Figure S18). During the experiments the light exposition was measured with an Oceans Optics (Dunedin, FL, USA) USB 4000 fiber optic spectrometer with an approximate resolution of 0.4 nm. All the experiments were performed twice. Results are presented as mean value of single experiments. Error bars represent the standard deviation of the repetitions.

3.5. Photocatalytic Degradation Experiments

The solutions of SMX were prepared in ultrapure water or river water, at the concentration of 1 mg/L (C_{SMX_0}). In the study, seven different photocatalysts were used: TiO_2, Pd/TiO_2 0.1% wt., Pd/TiO_2 0.5% wt., Pd/TiO_2 1.0% wt., Pt/TiO_2 0.1% wt., Pt/TiO_2 0.5% wt., and Pt/TiO_2 1.0% wt., where percentage corresponds to the level of TiO_2 surface modification with noble metal (w/w). Depending on the type of experiment, the SMX solution (C_{SMX_0} = 1 mg/L) was mixed in a flask with catalyst to the final concentration of catalyst (C_{cat}) of around 25 mg/L, 50 mg/L, 75 mg/L, and 120 mg/L. In order to reach adsorption equilibrium the flasks which were covered with aluminum foil were kept away from the sunlight for an hour. Afterwards, experimental solutions with catalyst were transferred to 50 mL transparent beakers and exposed to natural sunlight for 30 min. During this time, 1 mL samples were collected in amber glass containing 1 mL of ultrapure water at fixed time points. Subsequently samples were filtrated via syringe cellulose acetate filters (pore size 0.45 µm, Macherey-Nagel GmbH & Co. KG, Düren, Germany) and measured using liquid chromatography coupled with mass spectrometer (see Section 3.6.1) or high performance liquid chromatography with diode-array detector (see Section 3.6.2).

The effect of naturally occurring matrix on efficiency of photocatalytic degradation was tested using Alb river water (Karlsruhe, Germany) and Mondego river (Coimbra, Portugal) spiked with SMX (C_{SMX_0} = 1 mg/L), at catalyst concentration ~25 mg/L with a surface modification level of 1% wt. The physicochemical parameters of both investigated types of water are presented in SI Table S3.

3.6. Analytical Methods

3.6.1. Analysis by Liquid Chromatography Coupled with Tandem Mass Spectrometry (LC-MS/MS)

The SMX concentrations were measured using an Agilent 1290 Infinity II UHPLC system coupled to an Agilent 6470 Triple Quadrupole LC/MS system with an Agilent Jet Stream electrospray ionization source (Waldbronn, Germany). To minimize the variation of compound ionization during individual runs, samples were spiked with sulfamethoxazole-d_4 (internal standard) before injection for the calculation of the normalized area (i.e., the ratio between the peak area of the analyte of interest and the peak area of the internal standard of the corresponding parent compound). The separation was performed on an Agilent ZORBAX Eclipse Plus C-18 column (2.1 × 50 mm, 1.8 µm particle size). The elution was achieved with ultrapure water (A) and acetonitrile (B), both acidified with 0.05% formic acid at a flow rate of 400 µL/min using the following gradient program: time (min)/B (%); 0/5, 0.2/5, 4.2/95, 5.6/95, 5.8/5, 8.5/5. The injection volume was set to 5 µL and the temperature of column was set to 40 °C. The detection of positive ions was performed in dynamic multiple-reaction-monitoring mode (DynMRM). A detailed description of mass spectrometer settings is described in SI Tables S4 and S5. The data were analyzed using Agilent Technologies MassHunter Workstation Software Quantitative Analysis Version B.07.01 for QQQ.

3.6.2. Analysis by High Performance Liquid Chromatography with Diode Array Detector (HPLC-DAD)

Alternatively, in experiments performed in Portugal, SMX was quantified using high-performance liquid chromatograph (HPLC) UFLC Shimadzu (Kyoto, Japan), which was equipped with a diode array detector (DAD). The separation was performed using a Silia Chrom AQ C-18 column (4.6 × 250 mm, 5 µm particle size, 100A, Silicycle, Québec, Canada). The isocratic elution with acetonitrile and 11.5 mM solution of NaH_2PO_4 in ultrapure water, in the volumetric ratio 60/40 at a flow rate of 1 mL/min was applied. The temperature of the column compartment was set to 30 °C. The injection volume was 100 µL and SMX was quantified at the wavelength 255 nm.

3.6.3. Determination of Dissolved Organic Carbon (DOC)

To assess the degree of mineralization, dissolved organic carbon content was measured before and after the irradiation process using a Shimadzu Total Carbon Analyzer applying the catalytic oxidation method. The experiment was performed with Pd/TiO_2 and Pt/TiO_2 at the surface modification level of 1% with catalyst concentration ~25 mg/L in SMX aqueous solution of initial concentration of 1 mg/L.

3.7. Kinetics Description

For description of degradation kinetics, the pseudo-first order approach was used, in agreement with previous studies [25,50,51]. Pseudo-first order rate constants and half-lives were calculated. This approach was used both for the reactions in aqueous solutions and river water spiked with SMX.

3.8. Identification of TPs by LC-MS/MS

The search of TPs formed during the studied processes was performed based on the work of Gmurek et al. [46]. Ten potential TPs (SI Table S4) were used in the target analysis of samples irradiated as described in Section 3.5 using catalysts modified with 1% noble metal, at an initial concentration of ~25 mg/L. The same analytical method as previously explained in Section 3.6.1 was applied. The optimized MS/MS parameters for the TPs determination are collected in Table S3. Identification and semi-quantification of the targets was done using Agilent MassHunter Quantitative Analysis B.07.00 Software.

3.9. Toxicity Assessment

The toxicity of TPs formed during photocatalysis with Pd/TiO_2 and Pt/TiO_2 was assessed using plant *Lepidium sativum*, which was considered a bioindicator. SMX solution of concentration of 1 mg/L was irradiated as described in Section 3.5 with catalysts of 1% surface modification level and initial concentration ~25 mg/L. To increase the chance of high SMX removal and significant formation of TPs, the sun exposition was prolonged from 30 min (used for rest of the experiments) to 60 min. Toxic effects, expressed as the germination index (GI) [48] were compared with unirradiated SMX solution. Details concerning the test performance are explained elsewhere [25].

4. Conclusions

Our detailed characterization of catalysts showed that surface modification of TiO_2 with Pd and Pt significantly improved the absorption properties of the catalyst resulting in higher SMX abatement from aqueous solutions as compared with non-modified TiO_2. Results also indicated that the extend of surface modification plays a more important role in the case of modification with Pd than with Pt, partially due to the higher adsorption properties of Pd. On the other hand, the efficiency of the photocatalysis was affected more by initial concentration of Pt/TiO_2 as compared with Pd/TiO_2. Another interesting aspect of our study was the comparison of the effect of geographic location that showed higher abatement of SMX in pure solutions in Germany as compared with Portugal due to better irradiance conditions. However, despite worse irradiance conditions in Portugal, both Pd/TiO_2 and Pt/TiO_2 performed better in SMX degradation in Mondego river as compared with Alb river (i.e., k' values for Pd/TiO_2 and Pt/TiO_2 in Mondego river were around two times higher as compared with Alb water). Since the TOC concentration was comparable at the two studied locations, the differences in k' value resulted from the type of organic content and maybe from the presence of other water constituents.

The comparison of the rate constants of SMX degradation in various conditions led us to conclusion that modification with Pd gave better results than modification with Pt. The removal of SMX was faster with Pd/TiO_2 than with Pt/TiO_2, independent of the level of modification. On the other hand, when the same modification level was used, comparable rate constants were achieved which were 23.5 mg/L and 81.3 mg/L of Pd/TiO_2 and Pt/TiO_2, respectively. This superior effect of Pd/TiO_2 was also recognizable in the degradation process with river water samples. The TOC measurements showed that Pd/TiO_2 not only causes faster SMX degradation, but also slightly more efficient mineralization. Nevertheless, in both cases, the same TPs were formed, which substantially reduced the toxic effect towards *Lepidium sativum*. The differences in catalysts performance can be explained by their different optical properties. Since Pd/TiO_2 has lower bandgap as compared with Pt/TiO_2, (direct 2.92 eV and 3.18 eV, respectively) it requires lower energy for activation, and therefore it exhibits better characteristics in visible light range.

Despite the undeniable benefits of modification of TiO_2 with Pd and Pt, these types of modifications are expensive. An option to make the technology more economical feasible would be to recycle the catalysts, however, this issue was not in the scope of this study.

Supplementary Materials: The following are available online at http://www.mdpi.com/2073-4344/9/6/500/s1: Figure S1, characterization of noble metal-modified TiO_2 (**a**) SEM image of 1% Pd/TiO_2, (**b**) SEM image of 1% Pt/TiO_2; Figure S2, Characterization of Pd/TiO2 with SEM (a) 0.1 wt % Pd; (b) 0.5 wt % Pd; (c) 1 wt % Pd. Magnitude 5000x; Table S1, XRD characterization of Pd/Pt-TiO_2 used in the study, distribution of anatase and rutile phases, unit cell parameters and crystallite size of photocatalysts particles; Figure S3, LeBail refinement of room temperature powder X-ray diffraction data for (**a**) 1% Pt/TiO_2 and (**b**) 1% Pd/TiO_2; Figure S4, (**a**) adsorption capacity of selected catalysts with respect to SMX, (**b**) sorption of SMX on the TiO_2, Pt/TiO_2 and Pd/TiO_2 surface (C_{cat} = ~25 mg/L, modification level 1%); Figure S5, solar photocatalytic degradation of sulfamethoxazole using Pd/TiO_2 (C_{cat} = ~25 mg/L) at various modification levels; Figure S6, solar photocatalytic degradation of sulfamethoxazole using Pt/TiO_2 (C_{cat} = ~25 mg/L) at various modification levels; Figure S7, XPS spectra of modified TiO_2 (**a**) wide-scan survey spectrum of Pt/TiO_2 with insert of Ti 2p, (**b**) Pt(4f) XPS signals of Pt/TiO_2 1%, (**c**) wide-scan survey spectrum of Pd/TiO_2 with insert of Ti 2p, (**d**) Pd(3d) XPS signals of Pd/TiO_2 1%; Figure S8, solar photocatalytic degradation of sulfamethoxazole using Pd/TiO_2 (modification level 1%) at various initial concentration of catalysts; Figure S9, solar photocatalytic degradation of sulfamethoxazole using Pt/TiO_2 (modification level 1%) at various

initial concentration of catalysts; Figure S10, dependence of pseudo-first order rate constant on the concentration of noble metal used for SMX photodegradation; Figure S11, comparison of solar photocatalytic degradation of sulfamethoxazole using Pt/TiO_2 and Pd/TiO_2 (modification level 1%, C_{cat} = ~25 mg/L) in (**a**) Alb river water and (**b**) Mondego river water; Table S2, target analysis of TPs; Figure S12, MS^2 spectrum of sulfamethoxazole (SMX), precursor ion 254.0 m/z; Figure S13, MS^2 spectrum of 3-amino-5-methylisoxazole (3A5MI), precursor ion 99.1 m/z; Figure S14, MS^2 spectrum of N-hydroxy-sulfamethoxazole (N-OH-SMX), precursor ion 270.1 m/z; Figure S15, MS^2 spectrum of 4-nitroso-sulfamethoxazole (NO-SMX), precursor ion 265.9 m/z; Figure S16, MS^2 spectrum of 4-nitro-sulfamethoxazole (NO2-SMX), precursor ion 282.0m/z; Figure S17, degradation of SMX during photocatalysis with Pt/TiO_2 and Pd/TiO_2 (level of modification 1%, C_{cat} = ~25 mg/L). samples used for toxicity assessment; Figure S18, comparison of sunlight exposition in Portugal and Germany; Table S3, physico-chemical parameters of Alb river water and Mondego river water; Table S4, settings of mass spectrometer source; Table S5, optimized MS/MS parameters for determination of SMX and its TPs.

Author Contributions: Conceptualization, E.B. and M.G.; funding acquisition, H.H. and M.G.; investigation, E.B., J.F.G., R.C.M., R.M.Q.-F., and M.G.; methodology, E.B. and M.G.; resources, R.M.Q.-F. and H.H.; supervision, H.H.; writing—original draft, E.B.; writing—review and editing, E.B., J.F.G., R.C.M., R.M.Q.-F., H.H., and M.G. All authors read, revised and approved the manuscript.

Funding: This study was funded by the German Technical and Scientific Association for Gas and Water (DVGW). Marta Gmurek gratefully acknowledges German Academic Exchange Service DAAD (Deutscher Akademischer Austauschdienst) for financing the short-term research stay at KIT EBI Water Chemistry and Water Technology. Marta Gmurek acknowledges also financial support from the Mobility Plus Program (Project No. 1650/MOB/V/2017/0) funded by the Polish Ministry of Science and Higher Education (from 2018). João F. Gomes and Rui C. Martins gratefully acknowledge the Fundaçãopara a Ciênciae Tecnologia for the financial support under IFCT2014 Program (No. IF/00215/2014) with financing from the European Social Fund and the Human Potential Operational Programme.

Acknowledgments: The authors thank Katarzyna Bednarczyk and Marek Stelmachowski (Lodz University of Technology, Poland) for providing noble metal-modified TiO_2, Luís Miguel Moura Neves de Castro (CIEPQPF, Portugal) for providing the value of TOC in Mondego river, and Rafael Peschke and Matthias Weber (KIT, EBI Water Chemistry and Water Technology) for the laboratory assistance. The authors thank also Emília Quinta-Ferreira (CNC) Center for Neuroscience and Cell Biology and Department of Physics, University of Coimbra) for contribution in characterization of catalysts with SEM technique.

Conflicts of Interest: The authors declare no conflict of interest.

References

1. Bourgin, M.; Beck, B.; Boehler, M.; Borowska, E.; Fleiner, J.; Salhi, E.; Teichler, R.; von Gunten, U.; Siegrist, H.; McArdell, C.S. Evaluation of a full-scale wastewater treatment plant upgraded with ozonation and biological post-treatments: Abatement of micropollutants, formation of transformation products and oxidation by-products. *Water Res.* **2018**, *129*, 486–498. [CrossRef]
2. Luo, Y.; Guo, W.; Ngo, H.H.; Nghiem, L.D.; Hai, F.I.; Zhang, J.; Liang, S.; Wang, X.C. A review on the occurrence of micropollutants in the aquatic environment and their fate and removal during wastewater treatment. *Sci. Total Environ.* **2014**, *473–474*, 619–641. [CrossRef]
3. Rodriguez-Mozaz, S.; Chamorro, S.; Marti, E.; Huerta, B.; Gros, M.; Sànchez-Melsió, A.; Borrego, C.M.; Barceló, D.; Balcázar, J.L. Occurrence of antibiotics and antibiotic resistance genes in hospital and urban wastewaters and their impact on the receiving river. *Water Res.* **2015**, *69*, 234–242. [CrossRef]
4. Tran, N.H.; Reinhard, M.; Gin, K.Y.-H. Occurrence and fate of emerging contaminants in municipal wastewater treatment plants from different geographical regions-a review. *Water Res.* **2018**, *133*, 182–207. [CrossRef]
5. Gao, P.; Munir, M.; Xagoraraki, I. Correlation of tetracycline and sulfonamide antibiotics with corresponding resistance genes and resistant bacteria in a conventional municipal wastewater treatment plant. *Sci. Total Environ.* **2012**, *421-422*, 173–183. [CrossRef]
6. Bilińska, L.; Gmurek, M.; Ledakowicz, S. Textile wastewater treatment by aops for brine reuse. *Process Saf. Environ. Prot.* **2017**, *109*, 420–428. [CrossRef]
7. Kanakaraju, D.; Glass, B.D.; Oelgemöller, M. Advanced oxidation process-mediated removal of pharmaceuticals from water: A review. *J. Environ. Manag.* **2018**, *219*, 189–207. [CrossRef]
8. Miklos, D.B.; Remy, C.; Jekel, M.; Linden, K.G.; Drewes, J.E.; Hübner, U. Evaluation of advanced oxidation processes for water and wastewater treatment—A critical review. *Water Res.* **2018**, *139*, 118–131. [CrossRef]

9. Benotti, M.J.; Stanford, B.D.; Wert, E.C.; Snyder, S.A. Evaluation of a photocatalytic reactor membrane pilot system for the removal of pharmaceuticals and endocrine disrupting compounds from water. *Water Res.* **2009**, *43*, 1513–1522. [CrossRef]
10. Borowska, E.; Felis, E.; Żabczyński, S. Degradation of iodinated contrast media in aquatic environment by means of UV, UV/TiO_2 process, and by activated sludge. *Water Air Soil Pollut.* **2015**, *226*, 151. [CrossRef]
11. Carbajo, J.; Jiménez, M.; Miralles, S.; Malato, S.; Faraldos, M.; Bahamonde, A. Study of application of titania catalysts on solar photocatalysis: Influence of type of pollutants and water matrices. *Chem. Eng. J.* **2016**, *291*, 64–73. [CrossRef]
12. Mena, E.; Rey, A.; Beltrán, F.J. TiO_2 photocatalytic oxidation of a mixture of emerging contaminants: A kinetic study independent of radiation absorption based on the direct-indirect model. *Chem. Eng. J.* **2018**, *339*, 369–380. [CrossRef]
13. Chong, M.N.; Jin, B.; Chow, C.W.K.; Saint, C. Recent developments in photocatalytic water treatment technology: A review. *Water Res.* **2010**, *44*, 2997–3027. [CrossRef]
14. Lan, Y.; Lu, Y.; Ren, Z. Mini review on photocatalysis of titanium dioxide nanoparticles and their solar applications. *Nano Energy* **2013**, *2*, 1031–1045. [CrossRef]
15. Ribao, P.; Corredor, J.; Rivero, M.J.; Ortiz, I. Role of reactive oxygen species on the activity of noble metal-doped TiO_2 photocatalysts. *J. Hazard. Mater.* **2018**. [CrossRef]
16. Malato, S.; Fernández-Ibáñez, P.; Maldonado, M.I.; Blanco, J.; Gernjak, W. Decontamination and disinfection of water by solar photocatalysis: Recent overview and trends. *Catal. Today* **2009**, *147*, 1–59. [CrossRef]
17. Etacheri, V.; Di Valentin, C.; Schneider, J.; Bahnemann, D.; Pillai, S.C. Visible-light activation of TiO_2 photocatalysts: Advances in theory and experiments. *J. Photochem. Photobiol. C* **2015**, *25*, 1–29. [CrossRef]
18. Fagan, R.; McCormack, D.E.; Dionysiou, D.D.; Pillai, S.C. A review of solar and visible light active TiO_2 photocatalysis for treating bacteria, cyanotoxins and contaminants of emerging concern. *Mater. Sci. Semicond. Process.* **2016**, *42*, 2–14. [CrossRef]
19. Grabowska, E.; Marchelek, M.; Klimczuk, T.; Trykowski, G.; Zaleska-Medynska, A. Noble metal modified TiO_2 microspheres: Surface properties and photocatalytic activity under UV–Vis and visible light. *J. Mol. Catal. A* **2016**, *423*, 191–206. [CrossRef]
20. Lang, X.; Chen, X.; Zhao, J. Heterogeneous visible light photocatalysis for selective organic transformations. *Chem. Soc. Rev.* **2014**, *43*, 473–486. [CrossRef]
21. Sung-Suh, H.M.; Choi, J.R.; Hah, H.J.; Koo, S.M.; Bae, Y.C. Comparison of ag deposition effects on the photocatalytic activity of nanoparticulate TiO_2 under visible and uv light irradiation. *J. Photochem. Photobiol. A* **2004**, *163*, 37–44. [CrossRef]
22. Chen, H.-W.; Ku, Y.; Kuo, Y.-L. Effect of Pt/TiO_2 characteristics on temporal behavior of o-cresol decomposition by visible light-induced photocatalysis. *Water Res.* **2007**, *41*, 2069–2078. [CrossRef]
23. Guo, X.-W.; Hao, C.-H.; Wang, C.-Y.; Sarina, S.; Guo, X.-N.; Guo, X.-Y. Visible light-driven photocatalytic Heck reaction over carbon nanocoil supported Pd nanoparticles. *Catal. Sci. Technol.* **2016**, *6*, 7738–7743. [CrossRef]
24. Su, R.; Tiruvalam, R.; He, Q.; Dimitratos, N.; Kesavan, L.; Hammond, C.; Lopez-Sanchez, J.A.; Bechstein, R.; Kiely, C.J.; Hutchings, G.J.; Flemming, B. Promotion of phenol photodecomposition over TiO_2 using Au, Pd, and Au–Pd nanoparticles. *ACS Nano* **2012**, *6*, 6284–6292. [CrossRef] [PubMed]
25. Gomes, J.F.; Leal, I.; Bednarczyk, K.; Gmurek, M.; Stelmachowski, M.; Zaleska-Medynska, A.; Quinta-Ferreira, M.E.; Costa, R.; Quinta-Ferreira, R.M.; Martins, R.C. Detoxification of parabens using UV-A enhanced by noble metals—TiO_2 supported catalysts. *J. Environ. Chem. Eng.* **2017**, *5*, 3065–3074. [CrossRef]
26. Foszpańczyk, M.; Bednarczyk, K.; Drozdek, E.; Martins, R.C.; Ledakowicz, S.; Gmurek, M. Comparison of photocatalytic and photosensitized oxidation of paraben aqueous solutions under sunlight. *Water Air Soil Pollut.* **2018**, *229*, 362. [CrossRef]
27. Oros-Ruiz, S.; Zanella, R.; Prado, B. Photocatalytic degradation of trimethoprim by metallic nanoparticles supported on TiO_2-P25. *J. Hazard. Mater.* **2013**, *263*, 28–35. [CrossRef]
28. Ternes, T.; Joss, A. *Human Pharmaceuticals, Hormones and Fragrances. The Challenge of Micropollutants in Urban Water Management*; IWA Publishing: London, UK, 2006.

29. Ioannidou, E.; Frontistis, Z.; Antonopoulou, M.; Venieri, D.; Konstantinou, I.; Kondarides, D.I.; Mantzavinos, D. Solar photocatalytic degradation of sulfamethoxazole over tungsten—Modified TiO_2. *Chem. Eng. J.* **2017**, *318*, 143–152. [CrossRef]
30. Chiang, L.-F.; Doong, R.-A. Enhanced photocatalytic degradation of sulfamethoxazole by visible-light-sensitive TiO_2 with low Cu addition. *Sep. Purif. Technol.* **2015**, *156*, 1003–1010. [CrossRef]
31. Zanella, R.; Avella, E.; Ramírez-Zamora, R.M.; Castillón-Barraza, F.; Durán-Álvarez, J.C. Enhanced photocatalytic degradation of sulfamethoxazole by deposition of Au, Ag and Cu metallic nanoparticles on TiO_2. *Environ. Technol.* **2018**, *39*, 2353–2364. [CrossRef]
32. Bao, Y.; Lim, T.-T.; Zhong, Z.; Wang, R.; Hu, X. Acetic acid-assisted fabrication of hierarchical flower-like Bi_2O_3 for photocatalytic degradation of sulfamethoxazole and rhodamine B under solar irradiation. *J. Colloid Interface Sci.* **2017**, *505*, 489–499. [CrossRef]
33. Liu, S.-H.; Wei, Y.-S.; Lu, J.-S. Visible-light-driven photodegradation of sulfamethoxazole and methylene blue by Cu_2O/rGO photocatalysts. *Chemosphere* **2016**, *154*, 118–123. [CrossRef]
34. Grilla, E.; Petala, A.; Frontistis, Z.; Konstantinou, I.K.; Kondarides, D.I.; Mantzavinos, D. Solar photocatalytic abatement of sulfamethoxazole over Ag_3PO_4/WO_3 composites. *Appl. Catal. B* **2018**, *231*, 73–81. [CrossRef]
35. Leong, K.H.; Chu, H.Y.; Ibrahim, S.; Saravanan, P. Palladium nanoparticles anchored to anatase TiO_2 for enhanced surface plasmon resonance-stimulated, visible-light-driven photocatalytic activity. *Beilstein J. Nanotechnol.* **2015**, *6*, 428–437. [CrossRef]
36. Guayaquil-Sosa, J.F.; Serrano-Rosales, B.; Valadés-Pelayo, P.J.; de Lasa, H. Photocatalytic hydrogen production using mesoporous TiO_2 doped with pt. *Appl. Catal. B* **2017**, *211*, 337–348. [CrossRef]
37. Guayaquil-Sosa, J.F.; Calzada, A.; Serrano, B.; Escobedo, S.; De Lasa, H. Hydrogen production via water dissociation using Pt–TiO_2 photocatalysts: An oxidation–reduction network. *Catalysts* **2017**, *7*, 324. [CrossRef]
38. Ibhadon, O.A.; Fitzpatrick, P. Heterogeneous photocatalysis: Recent advances and applications. *Catalysts* **2013**, *3*, 189–218. [CrossRef]
39. Bednarczyk, K.; Stelmachowski, M.; Gmurek, M. The influence of process parameters on photocatalytic hydrogen production. *Environ. Prog. Sustain. Energy* **2019**, *38*, 680–687. [CrossRef]
40. Orton, J. *The Story of Semiconductors*; Oxford University Press: New York, NY, USA, 2004.
41. Wang, Y.; Lai, Q.; Zhang, F.; Shen, X.; Fan, M.; He, Y.; Ren, S. High efficiency photocatalytic conversion of CO_2 with H_2O over Pt/TiO_2 nanoparticles. *RSC Adv.* **2014**, *4*, 44442–44451. [CrossRef]
42. Michaelson, H.B. The work function of the elements and its periodicity. *J. Appl. Phys.* **1977**, *48*, 4729–4733. [CrossRef]
43. García-Zaleta, D.S.; Torres-Huerta, A.M.; Domínguez-Crespo, M.A.; García-Murillo, A.; Silva-Rodrigo, R.; López González, R. Influence of phases content on Pt/TiO_2, Pd/TiO_2 catalysts for degradation of 4-chlorophenol at room temperature. *J. Nanomater.* **2016**, *2016*, 15.
44. Sakthivel, S.; Shankar, M.V.; Palanichamy, M.; Arabindoo, B.; Bahnemann, D.W.; Murugesan, V. Enhancement of photocatalytic activity by metal deposition: Characterisation and photonic efficiency of Pt, Au and Pd deposited on TiO_2 catalyst. *Water Res.* **2004**, *38*, 3001–3008. [CrossRef]
45. Abellán, M.N.; Bayarri, B.; Giménez, J.; Costa, J. Photocatalytic degradation of sulfamethoxazole in aqueous suspension of TiO_2. *Appl. Catal. B* **2007**, *74*, 233–241. [CrossRef]
46. Gmurek, M.; Horn, H.; Majewsky, M. Phototransformation of sulfamethoxazole under simulated sunlight: Transformation products and their antibacterial activity toward *Vibrio fischeri*. *Sci. Total Environ.* **2015**, *538*, 58–63. [CrossRef]
47. Schymanski, E.L.; Jeon, J.; Gulde, R.; Fenner, K.; Ruff, M.; Singer, H.P.; Hollender, J. Identifying small molecules via high resolution mass spectrometry: Communicating confidence. *Environ. Sci. Technol.* **2014**, *48*, 2097–2098. [CrossRef]
48. Trautmann, N.; Krasny, M. *Composting in the Classroom*; Nature Science Foundation; Cornell Waste Management Institute; Cornell Center for the Environment: New York, NY, USA, 1997.
49. Majewsky, M.; Wagner, D.; Delay, M.; Bräse, S.; Yargeau, V.; Horn, H. Antibacterial activity of sulfamethoxazole transformation products (TPs): General relevance for sulfonamide tps modified at the *para* position. *Chem. Res. Toxicol.* **2014**, *27*, 1821–1828. [CrossRef]

50. Borowska, E.; Felis, E.; Kalka, J. Oxidation of benzotriazole and benzothiazole in photochemical processes: Kinetics and formation of transformation products. *Chem. Eng. J.* **2016**, *304*, 852–863. [CrossRef]
51. Velegraki, T.; Hapeshi, E.; Fatta-Kassinos, D.; Poulios, I. Solar-induced heterogeneous photocatalytic degradation of methyl-paraben. *Appl. Catal. B* **2015**, *178*, 2–11. [CrossRef]

© 2019 by the authors. Licensee MDPI, Basel, Switzerland. This article is an open access article distributed under the terms and conditions of the Creative Commons Attribution (CC BY) license (http://creativecommons.org/licenses/by/4.0/).